



**HAL**  
open science

## Dilution effects on ultrafine particle emissions from Euro 5 and Euro 6 diesel and gasoline vehicles

Cédric Louis, Yao Liu, Simon Martinet, B d'Anna, Alvaro Martinez Valiente, Antoinette Boreave, Badr R'Mili, Patrick Tassel, Pascal Perret, Michel Andre

### ► To cite this version:

Cédric Louis, Yao Liu, Simon Martinet, B d'Anna, Alvaro Martinez Valiente, et al.. Dilution effects on ultrafine particle emissions from Euro 5 and Euro 6 diesel and gasoline vehicles. *Atmospheric Environment*, 2017, 169, pp.80-88. 10.1016/j.atmosenv.2017.09.007 . hal-01635462

**HAL Id: hal-01635462**

**<https://hal.science/hal-01635462v1>**

Submitted on 20 Mar 2019

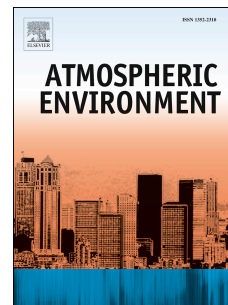
**HAL** is a multi-disciplinary open access archive for the deposit and dissemination of scientific research documents, whether they are published or not. The documents may come from teaching and research institutions in France or abroad, or from public or private research centers.

L'archive ouverte pluridisciplinaire **HAL**, est destinée au dépôt et à la diffusion de documents scientifiques de niveau recherche, publiés ou non, émanant des établissements d'enseignement et de recherche français ou étrangers, des laboratoires publics ou privés.

# Accepted Manuscript

Dilution effects on ultrafine particle emissions from Euro 5 and Euro 6 diesel and gasoline vehicles

Cédric Louis, Yao Liu, Simon Martinet, Barbara D'Anna, Alvaro Martinez Valiente, Antoinette Boreave, Badr R'Mili, Patrick Tassel, Pascal Perret, Michel André



PII: S1352-2310(17)30589-7

DOI: [10.1016/j.atmosenv.2017.09.007](https://doi.org/10.1016/j.atmosenv.2017.09.007)

Reference: AEA 15545

To appear in: *Atmospheric Environment*

Received Date: 8 March 2017

Revised Date: 22 August 2017

Accepted Date: 3 September 2017

Please cite this article as: Louis, Cé., Liu, Y., Martinet, S., D'Anna, B., Valiente, A.M., Boreave, A., R'Mili, B., Tassel, P., Perret, P., André, M., Dilution effects on ultrafine particle emissions from Euro 5 and Euro 6 diesel and gasoline vehicles, *Atmospheric Environment* (2017), doi: 10.1016/j.atmosenv.2017.09.007.

This is a PDF file of an unedited manuscript that has been accepted for publication. As a service to our customers we are providing this early version of the manuscript. The manuscript will undergo copyediting, typesetting, and review of the resulting proof before it is published in its final form. Please note that during the production process errors may be discovered which could affect the content, and all legal disclaimers that apply to the journal pertain.

## Dilution effects on ultrafine particle emissions from Euro 5 and Euro 6 diesel and gasoline vehicles

Cédric Louis <sup>a,b</sup>, Yao Liu <sup>a,\*</sup>, Simon Martinet <sup>a</sup>, Barbara D'Anna <sup>c</sup>, Alvaro Martinez Valiente <sup>c</sup>,  
Antoinette Boreave <sup>c</sup>, Badr R'Mili <sup>c</sup>, Patrick Tassel <sup>a</sup>, Pascal Perret <sup>a</sup>, Michel André <sup>a</sup>

<sup>a</sup> Univ Lyon, IFSTTAR, AME, LTE, F-69675, LYON, France

<sup>b</sup> French Environment and Energy Management Agency, ADEME, 49004 Angers, France

<sup>c</sup> IRCELYON – UMR 5256 CNRS – Université de Lyon, 69626 Villeurbanne, France

\* Corresponding author: [yao.liu@ifsttar.fr](mailto:yao.liu@ifsttar.fr), 25 avenue François Mitterrand, 69675 Bron, France

### Abstract

Dilution and temperature used during sampling of vehicle exhaust can modify particle number concentration and size distribution. Two experiments were performed on a chassis dynamometer to assess exhaust dilution and temperature on particle number and particle size distribution for Euro 5 and Euro 6 vehicles. In the first experiment, the effects of dilution (ratio from 8 to 4000) and temperature (ranging from 50 °C to 150 °C) on particle quantification were investigated directly from tailpipe for a diesel and a gasoline Euro 5 vehicles. In the second experiment, particle emissions from Euro 6 diesel and gasoline vehicles directly sampled from the tailpipe were compared to the constant volume sampling (CVS) measurements under similar sampling conditions. Low primary dilutions (3–5) induced an increase in particle number concentration by a factor of 2 compared to high primary dilutions (12–20). Low dilution temperatures (50 °C) induced 1.4–3 times higher particle number concentration than high dilution temperatures (150 °C). For the Euro 6 gasoline vehicle with direct injection, constant volume sampling (CVS) particle number concentrations were higher than after the tailpipe by a factor of 6, 80 and 22 for Artemis urban, road and motorway, respectively. For the same vehicle, particle size distribution measured after the tailpipe was centred on 10 nm, and particles were smaller than the ones measured after CVS that was centred between 50 nm and 70 nm. The high particle concentration ( $\approx 10^6$  #/cm<sup>3</sup>) and the growth of diameter, measured in the CVS, highlighted aerosol transformations, such as nucleation, condensation and coagulation occurring in the sampling system and this might have biased the particle measurements.

### Keywords

Gasoline and diesel emissions; CVS; Tailpipe; Dilution; Temperature; Ultrafine particle; Nucleation; Condensation; Coagulation

### Abbreviations

G-DI	Gasoline with Direct Injection	DPF	Diesel Particulate Filter
cat	Catalysed Filter	PMP	Particle Measurement Programme
CVS	Constant Volume Sampler	FPS	Fine Particle Sampler
NO <sub>x</sub>	Nitrogen Oxides	NO <sub>2</sub>	Nitrogen Dioxide
NO	Nitric Oxide	PN	Particle Number
CPC	Condensation Particle Counter	ELPI	Electrical Low Pressure Impactor
SMPS	Scanning Mobility Particle Sizer	FMPS	Fast Mobility Particle Sizer Spectrometer
HEPA	high-efficiency particulate air		

## 40 1 Introduction

41 Vehicle exhaust emissions represent a major source of particle matter in urban environments.  
42 On regional and global scales, atmospheric particles play an important role in human health and  
43 climate change (Ning, 2010; Kulmala et al., 2000; Pope III, 2000). Particles emitted from diesel and  
44 gasoline engines are ultrafine particles with size ranges of 20–130 nm and 20–60 nm, respectively  
45 (Karjalainen et al., 2014; Morawska et al., 2008; Burtscher 2005; Jamriska et al., 2004). The ultrafine  
46 particles represent only 0.1–10% of the total particulate mass, but it might represent more than 90% of  
47 the total particle number (Giechaskiel et al., 2010; Kittelson, 1998). Particle emission depends on the  
48 engine technology, fuel and aftertreatment devices. Liang et al. (2013) and Köhler (2013) showed that  
49 the gasoline direct injection (G-DI) technology induced an increase in the particle number  
50 concentration compared to the standard gasoline passenger cars. Moreover, the dilution process  
51 (dilution ratio, dilution gas temperature and sampling residence time) has been established as a factor  
52 influencing ultrafine particle formation (Manoukian et al., 2016; Wei et al., 2016; Ranjan et al., 2012;  
53 Fujitani et al., 2012; Mamakos and Martini, 2011; Grieshop et al., 2009a; Vouitsis et al., 2008;  
54 Rönkkö et al., 2006; Mathis et al. 2004). After the tailpipe, the exhaust undergoes high and fast  
55 atmospheric dilution ratio that could reach up from 1000 to 4000 in 1–3 s (Fujitani et al., 2012; Zhang  
56 and Wexler, 2004). The exhaust temperature (around 200 °C) decreases rapidly at ambient  
57 temperature level within few seconds after emission due to the high dilution ratio. The rapid decrease  
58 in temperature has significant implications in terms of thermodynamics of particles and semi-volatile  
59 compounds (Kim et al., 2016; Huang et al., 2014; May et al., 2013; Wang and Zhang, 2012; Kozawa et  
60 al., 2012; Mamakos and Martini, 2011; Casati et al., 2007; Morawska et al., 2008; Zhang et al., 2004)  
61 leading to a drastic change in particle number concentration and size distribution (Huang et al., 2014;  
62 Wang and Zhang, 2012; Uhrner et al., 2011; Grieshop 2009b). Although several recent studies have  
63 focused on that issue, uncertainties still remain regarding the experimental determination of ultrafine  
64 particle emissions from vehicle exhaust and the impact of dilution and temperature during their  
65 sampling (Wei et al., 2016; Manoukian et al., 2016; Ranjan et al., 2012; Fujitani et al., 2012; Grieshop  
66 et al., 2009a).

67 Particle number concentration is measured through a specific protocol, derived from the  
68 Particle Measurement Program (PMP) through the full-flow Constant Volume Sampler (CVS). This  
69 protocol requires the removal of the volatile phase by the dilution stage (150 °C) and a heated tube (at  
70 300–400 °C). The PMP approach only regulates the non-volatile fraction of particles in order to  
71 exclude the possible confounding of measurement data by low volatility hydrocarbons manifesting as  
72 a nucleation mode present below 20 nm that highly depends on the sampling conditions (Giechaskiel  
73 et al., 2008). In the atmosphere, the concentration of aerosols changes rapidly in the first seconds after  
74 emission with condensation phenomenon and presence of SVOCs, which strongly depend on the  
75 exhaust sampling (length of the sampling line, dilution factor, temperature, etc.) (Albriet et al., 2010).  
76 Several studies showed that the ultrafine particle number concentration directly measured from the  
77 tailpipe was significantly different than those from the CVS (Kim et al., 2016; Giechaskiel et al., 2010,  
78 2007; Mathis et al., 2005). Giechaskiel et al. (2010) showed that deceleration (from 140 km/h to 120  
79 km/h) induced a higher particle number concentration with higher mean diameter than acceleration  
80 (from 90 km/h to 120 km/h) with a Euro 3 diesel vehicle without particulate filter. This observation is  
81 in contrast with their previous work (Giechaskiel et al., 2007), which reported a lower particle number  
82 concentration during deceleration than during acceleration. This contradiction can be explained by  
83 differences in sampling systems. According to Giechaskiel et al. (2007), particles were sampled  
84 directly from the tailpipe, while in Giechaskiel et al. (2010), particles were sampled from the CVS. As  
85 mentioned by Giechaskiel et al. (2014), the CVS dilution tunnel has several disadvantages such as the  
86 inability to control the dilution ratio and the dilution temperature, a long sampling path and a long

87 residence time. This dilution system favours nucleation, condensation and coagulation that could  
88 induce the new particle formation or the modification of the particle size distribution.

89 Based on this evidence, the particle measurement directly from the tailpipe was considered as  
90 a complementary sampling method to CVS in order to understand the sampling condition impacts on  
91 particle number concentration. This work aimed to investigate the impacts of dilution and temperature  
92 on particle emissions after a CVS tunnel system and directly from the tailpipe with Euro 5 and Euro 6  
93 vehicles. Particle number and size distribution between the CVS and the tailpipe were compared under  
94 similar dilution conditions to investigate the processes occurring in the dilution tunnel with the Euro 6  
95 G-DI vehicle. Finally, we discussed the nucleation, condensation and coagulation phenomena  
96 observed into the CVS dilution system.

## 97 2 Materials and methods

### 98 2.1 Vehicle characteristics

99 Four currently in-use vehicles were studied: a Euro 5 gasoline with direct injection system (G-  
 100 DI), and Euro 5 diesel with catalysed particulate filter (DPF cat), a Euro 6 G-DI and a Euro 6 DPF cat.  
 101 Technical characteristics of the tested vehicles are shown in Table 1. All the tested vehicles were  
 102 private vehicles to be as representative as possible of the state of the current French fleet. All  
 103 experiments were conducted using commercial fuel (sulphur content less than 10 ppm) pumped from  
 104 the same petrol station to minimize variability of fuel composition and its impact on emissions.

105 Table 1. Technical characteristics of the tested vehicles.

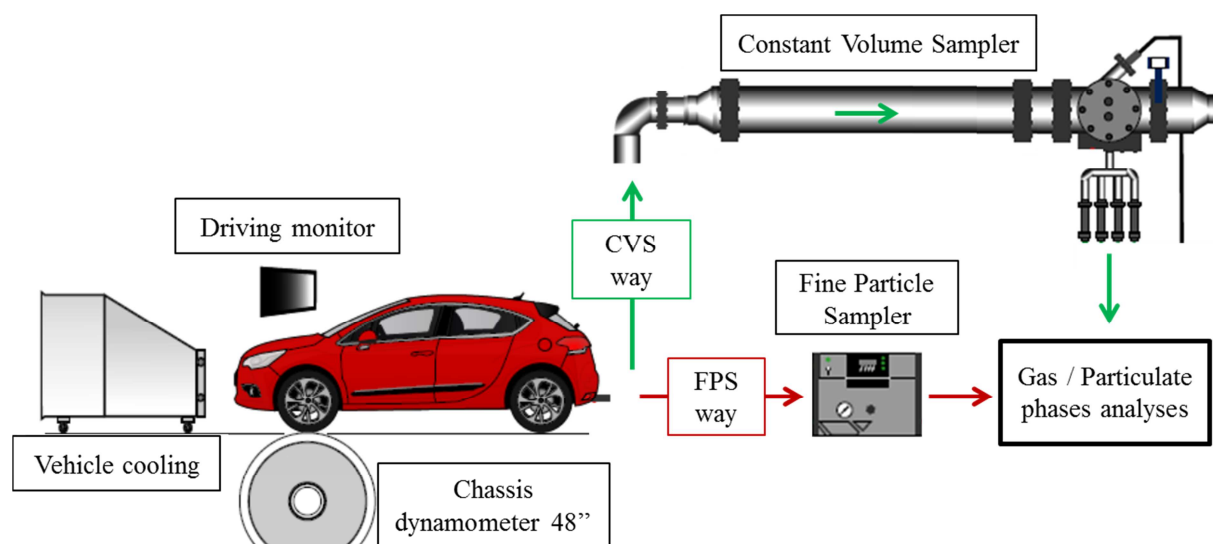
Vehicle	No. 1	No. 2	No. 3	No. 4
<b>Size class</b>	1.2	1.5	1.0	1.5
<b>Technology</b>	G-DI*	Diesel	G-DI*	Diesel
<b>Standard</b>	Euro5	Euro5	Euro 6	Euro 6
<b>Empty weight (kg)</b>	1320	1090	864	1087
<b>Mileage (km)</b>	25844	87073	2164	4700
<b>Gearbox type</b>	Manual (5)	Manual (5)	Manual (5)	Manual (5)
<b>Registration date</b>	27/02/2014	17/02/2012	11/12/2015	31/12/2015
<b>Test date</b>	31/03/2015	15/04/2015	29/03/2016	11/04/2016
<b>Catalyst</b>	Three-way	Oxidation	Three-way	Oxidation
<b>Filter</b>	No	Catalysed DPF <sup>§</sup>	No	Catalysed DPF <sup>§</sup>

106 \* G-DI: Gasoline with direct injection system

107 <sup>§</sup> DPF: Diesel Particulate Filter

### 108 2.2 Experimental set-up

109 Emission measurements were performed on the chassis dynamometer at the Transports and  
 110 Environment Laboratory (LTE) of the French Institute of Science and Technology for Transport,  
 111 Development and Networks (IFSTTAR). The chassis dynamometer was composed of a 48-inch roller  
 112 on which the drive wheels of the vehicle were placed. The dynamometer resisted to the vehicle rolling  
 113 to simulate the road resistance, which was calculated based on road laws for each vehicle. The schema  
 114 of the experimental setup is shown in Figure 1. Vehicle exhausts were sampled through two different  
 115 ways: one directly at the tailpipe, diluted by the fine particle sampler (FPS) and the other through the  
 116 CVS. Exhaust sampling from these two systems was diluted with filtered ambient air system.



117

118 Figure 1. Schema of the experimental setup; the green arrows represent the CVS way and the red  
119 arrows represent the direct tailpipe way with FPS dilution.

## 120 2.2.1 Dilution systems

### 121 • Constant Volume Sampler (CVS)

122 Exhaust emissions measured using a CVS system were diluted with filtered ambient air (4 filters in  
123 series including M6-F7-F9, M5, F7 EN-779-2012 filters, a HEPA H13 EN1822-2009 filter and a  
124 cylindrical cartridge of charcoal scrubber). This filtered air allowed compensating the flow rate  
125 variations related to the exhaust flow fluctuations and keeping a constant volume sampling. The  
126 mixture air/exhaust went through the dilution tunnel, and then was monitored by different on-line gas  
127 and particulate phase analysers.

### 128 • Fine Particle Sampler (FPS)

129 A Fine Particle Sampler (FPS 4000, Dekati Ltd) was used for direct tailpipe dilution. The exhaust  
130 dilution was carried out in two stages: a primary dilution, close to the sampling point with controlled  
131 temperature and a secondary dilution as ejector type diluter, located downstream of the primary  
132 dilution and which adjusted the primary dilution to provide the total dilution. The FPS enabled the  
133 control of several dilution parameters such as sampling flow, primary dilution, total dilution and  
134 temperature.

## 135 2.2.2 Experimental protocol

136 Dilution and temperature effects were studied with two Euro 5 vehicles: gasoline (No. 1) and  
137 diesel (No. 2). The vehicles were tested with two Artemis cycles (motorway and urban) (André, 2004)  
138 and at 70 km/h steady speed. The particles were sampled from the tailpipe after the FPS dilution with  
139 or without VKL diluters (depending on the total dilution tested). The FPS dilution temperatures were  
140 set at 50°C, 100°C, and 150°C and the total dilution ratios were 30, 100, 400, 1000, 2000 and 4000 for  
141 gasoline and 8, 12, 16, 30, 100, 400, 1000, 2000, 4000 for diesel. Each experimental condition was  
142 repeated three times.

143 To compare the tailpipe emissions with the CVS measurements, the Euro 6 gasoline (No.3)  
144 and the diesel (No.4) vehicles were tested with Artemis road, motorway and urban driving conditions.  
145 The detailed driving cycles with repeated tests and sampling conditions were shown in Table 2. The  
146 CVS operated at a total flow rate of 11 m<sup>3</sup>/min for the Artemis motorway cycle and 9 m<sup>3</sup>/min for the  
147 other driving cycles. The average CVS dilution ratios ranged between 13 and 60 for the gasoline  
148 vehicle and between 22 and 77 for the diesel vehicle, with a dilution temperature at 35 °C. At the



149 tailpipe the FPS primary dilution was set at 36°C to reproduce similar dilution and temperature  
150 conditions as in the CVS.

151 Table 2. Detailed driving cycles with test number and sampling conditions for the FPS and the CVS  
152 with Euro 6 G-DI (No.3) and Euro 6 diesel DPF cat (No.4) vehicles.

Vehicles	Euro 6 G-DI (No. 3)				Euro 6 diesel DPF cat (No. 4)			
	Repeated cycles	Repeated number	CVS dilution	Total tailpipe dilution	Primary dilution	Repeated number	CVS dilution	Total tailpipe dilution
Road	9	33	35	22	9	51	54	25
Urban	10	60	59	25	10	77	88	27
Motorway	6	13	15	12	6	22	18	17

### 153 2.3 Analytical methods

#### 154 2.3.1 Regulated compound analysis

155 Regulated compounds, such as carbon oxide (CO), carbon dioxide (CO<sub>2</sub>), total hydrocarbons  
156 (THC), nitric oxide (NO) and nitrogen oxides (NO<sub>x</sub>) were monitored using a Horiba emission  
157 measurement system (CO and CO<sub>2</sub> by non-dispersive infrared, THC by flame ionization detection, NO  
158 and NO<sub>x</sub> by chemiluminescence). The NO<sub>2</sub> concentration was determined by subtracting NO from  
159 NO<sub>x</sub>. Regulated compounds were monitored to ensure that vehicles had regular emission behaviours  
160 with respect to their category and to detect any abnormalities that could introduce bias in the  
161 measurements.

#### 162 2.3.2 Particulate phase analysis

163 The particle number concentration and the size distribution were measured by a Fast Mobility  
164 Particle Sizer Spectrometer (FMPS, model 3091 TSI). Particles went through a cyclone with a 1µm cut  
165 off and an electrical diffusion charger. The particle number concentration from 5.6 nm to 560 nm is  
166 determined by measuring the electrical current collected on a series of electrodes. Data were collected  
167 every second at 8 L/min. The quantification limit depended on the particle size: for 5.6 nm the  
168 maximum limit was 10<sup>7</sup> #/cm<sup>3</sup> and the minimum limit was 100 #/cm<sup>3</sup>. Particle size number distribution  
169 was also characterised using an Electrical Low Pressure Impactor (ELPI, Dekati). The ELPI measured  
170 the particle number distribution in the 7 nm to 4 µm range with 12 filter stages. The operating flow  
171 rate of the ELPI was set at 10 L/min with a sampling period of 1s. The quantification limits ranged  
172 from 250 to 7×10<sup>7</sup> #/cm<sup>3</sup> for particles with a diameter between 7 nm and 4 µm and from 0.1 to 2×10<sup>4</sup>  
173 #/cm<sup>3</sup> for particles with a diameter greater than 4 µm. A Condensation Particle Counter (CPC, model  
174 3775 TSI) was used for total particle number concentration. The CPC contained a butanol  
175 condensation chamber that enabled the detection of particles greater than 4 nm (particle size cut 50%).  
176 The operating flow rate of CPC was set at 1.5 L/min. The experimental data were collected every  
177 second with a concentration ranging from 0 to 10<sup>7</sup> #/cm<sup>3</sup>.

178 The Particle Measurement Programme has been proposed as a regulatory approach for  
179 measuring particle numbers for Euro 5 and Euro 6 vehicles, with a 50% cut-point size of 23 nm.  
180 However, most particles emitted by the tested vehicles in our previous experiments were ultrafine  
181 particles with diameters below 23 nm, especially during the Artemis motorway driving cycle and



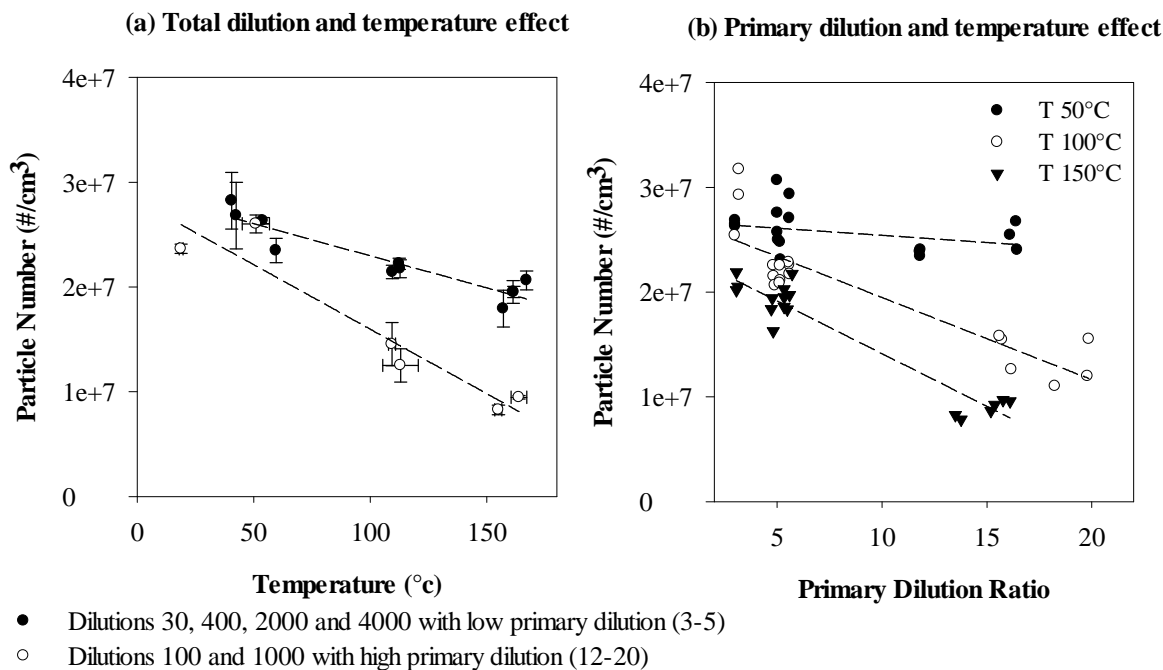
182 particulate filter regeneration (Louis et al., 2016). In order to have the most complete information on  
183 total particle number emissions including particles smaller than 23 nm, and to compare it with direct  
184 tailpipe emission, we did not fully follow the PMP protocol in this study. However the CVS tunnel  
185 was conditioned according the latest regulatory requirement in Europe with heated air dilution at  
186 35°C. Furthermore, by considering the volatile fraction of particles, the standard variations of particle  
187 number concentration with six repeated tests, ranged from 7 to 11%.

ACCEPTED MANUSCRIPT

### 188 3 Results and discussion

#### 189 3.1 Dilution and temperature effects

190 For the Euro 5 gasoline vehicle, the exhaust was sampled directly from the tailpipe at different  
191 total dilution ratios through the FPS (at 30, 100, 400, 1000, 2000 and 4000). The total dilution ratios at  
192 30, 400, 2000 and 4000 were obtained with low primary dilution ratios between 3 and 5, while the  
193 total dilution at 100 and 1000 were obtained with high primary dilution ratios between 12 and 20.  
194 Figure 2a showed the particle number concentration with the total dilution ratios between 30 and 4000  
195 as function of the dilution temperature at 50, 100 and 150 °C during motorway driving condition. We  
196 observed that the temperature played an important role on particle concentrations. According to  
197 Beckers et al. (2009), low temperature (50 °C) induced 1.4 to 3 times more PN than high temperature  
198 (150 °C) for all tested dilution ratios. The PN concentrations were classified into two groups: black  
199 dots for total dilution of 30, 400, 2000 and 4000 characterized by a low primary dilution (3–5); white  
200 empty dots for the total dilution at 100, 1000 with high primary dilution (12–20). These latter total  
201 dilutions induced less particle emissions than dilution at 30, 400, 2000 and 4000 (Figure 2a). This can  
202 be explained by the fact that dilution ratios 100 and 1000 were achieved using high primary dilution  
203 ratio and it emphasised the key role of the primary dilution ratio. Figure 2b showed the particle  
204 number emissions from a gasoline vehicle as function of the primary dilution (3–20) under motorway  
205 driving condition with three primary dilution temperatures (50, 100 and 150°C). The particle number  
206 concentration was corrected taking into account the dilution factors. At low primary dilution (3–5)  
207 with the three tested dilution temperatures, PN concentrations were at  $2\text{--}3 \times 10^7 \text{ \#/cm}^3$ . For these  
208 sampling conditions, PN concentration did not depend on the dilution gas temperature. At high  
209 primary dilution conditions (12–20), PN concentration decreased with the increase in temperature. PN  
210 emissions were about 2 times lower (at  $1\text{--}1.5 \times 10^7 \text{ \#/cm}^3$ ) at 100°C and 150°C than at 50°C. For the  
211 same temperature at 100 and 150 °C, the PN concentration decreased with the increase in the primary  
212 dilution ratio. These results were in agreement with the ones reported by Casati et al. (2007) for Euro3  
213 diesel passenger cars. Their results indicated that the low primary dilution and the low dilution  
214 temperature of gas might promote the measurement bias. They recommended setting the sampling  
215 system at a high primary dilution and high dilution temperature to minimise those bias. For the Euro 5  
216 diesel vehicle, PN emissions were low due to the high filtration efficiency of the diesel particulate  
217 filter (DPF). The particle number concentrations were lower than the detection limit of the instrument  
218 for most of the dilution conditions and were not presented.



219  
 220 Figure 2. Total dilution and temperature effects (a) and primary dilution and temperature effects (b)  
 221 for the gasoline Euro 5 vehicle (No. 1) during the motorway driving conditions, at 50°C, 100°C and  
 222 150°C. The particle number emissions are corrected taking into account of the dilution factors. For the  
 223 figure 2a, the black dots show total dilution ratios at 30, 400, 2000 and 4000 with low primary dilution  
 224 (3–5) and the white dots show total dilution ratios at 100 and 1000 with high primary dilution (12–20).

### 225 3.2 Euro 6 G-DI particle characterisation tailpipe / CVS

226 PN emissions measured from the tailpipe have also been compared with CVS measurements for  
 227 two Euro 5 vehicles under Artemis motorway cycle. Statistically significant differences in PN  
 228 concentration have been observed between these two sampling systems. Particle size distribution was  
 229 unimodal and centred at 20 nm after the tailpipe (FPS sampling system) and at more than 60 nm after  
 230 the CVS. However, different analysers have been used for the PN quantification at the tailpipe (with  
 231 an ELPI) and after the CVS (with a SMPS) due to experimental organisation and constraints.  
 232 Therefore, in order to better understand the physical processes occurring in the sampling systems, with  
 233 their impact on PN measurement, two Euro 6 gasoline and diesel vehicles have been tested. The PN  
 234 concentrations have been followed by a FMPS after the tailpipe and after the CVS with Artemis  
 235 Urban, Road and Motorway cycles. Primary dilution at 20 was chosen to the tailpipe dilution in order  
 236 to minimise the PN concentration measurement bias.

#### 237 3.2.1 Particle concentration comparison between tailpipe and CVS

238 Due to the high efficiency of the diesel particulate filter, PN emission from the Euro 6 diesel  
 239 vehicle was lower than the analyser detection limit. Therefore, only gasoline emissions were presented  
 240 and discussed here. Table 3 showed the average particle number concentrations for Euro 6 gasoline G-  
 241 DI for the Artemis urban, road and motorway driving cycles. The concentrations reported were  
 242 average values of several repeated cycles for each driving condition. The PN measurement after CVS  
 243 and tailpipe were performed under similar total dilution and temperature conditions (Table 2). PN  
 244 concentrations from CVS were higher than at tailpipe by a factor of 6, 80 and 22 for Artemis urban,  
 245 road and motorway, respectively. Highest discrepancies were observed under Artemis road cycle.  
 246 Unfortunately, we did not find an explication, since the tests were repeated 5 and 3 times after CVS  
 247 and exhaust, respectively, which showed similar result.

248  
 249

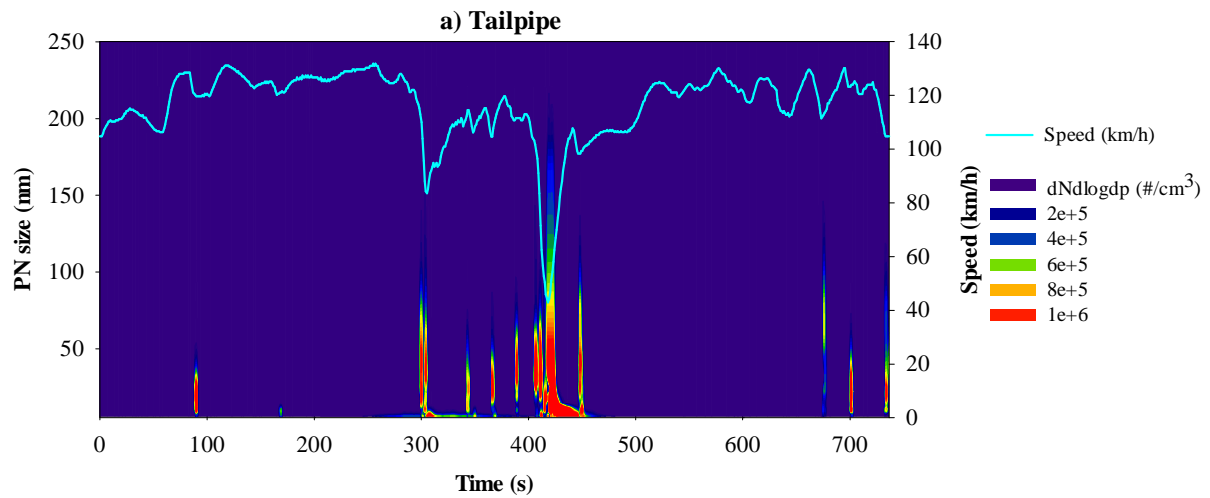
Table 3. Average particle number concentration for G-DI Euro 6 vehicle.

Particle concentration ( $\#/cm^3$ ) G-DI Euro 6						
Driving cycle		Start	CVS	Tests Number	Exhaust	Tests Number
Artemis	urban	hot start	$(9 \pm 5) \times 10^4$	7	$(1.4 \pm 0.6) \times 10^4$	3
Artemis	road	hot start	$(2.3 \pm 0.4) \times 10^6$	5	$(3 \pm 2) \times 10^4$	3
Artemis	motorway	hot start	$(2.2 \pm 0.1) \times 10^7$	3	$(1.0 \pm 0.3) \times 10^6$	3

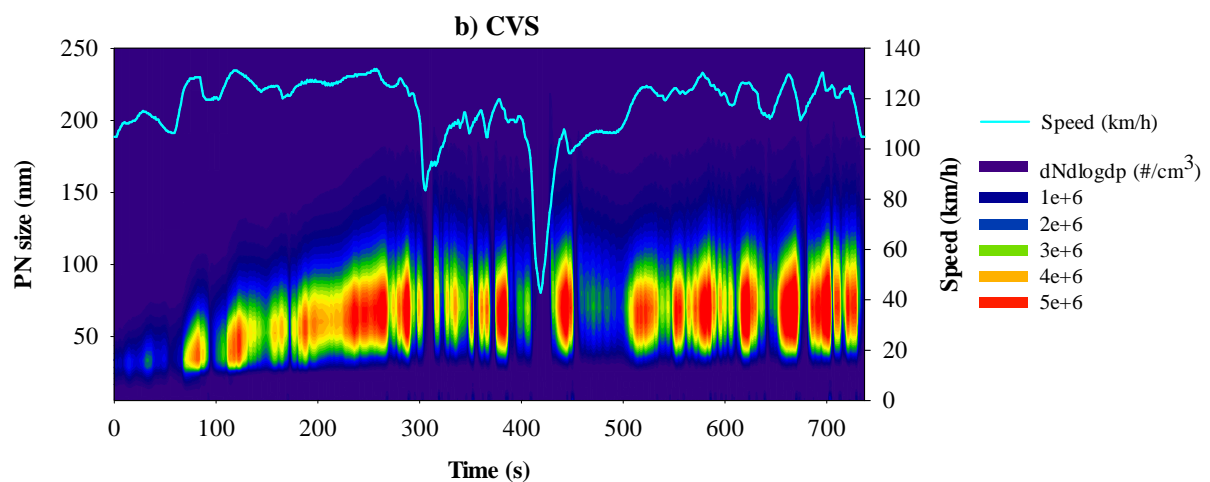
250  
 251  
 252  
 253  
 254  
 255  
 256  
 257  
 258  
 259  
 260

### 3.2.2 Particle size distribution comparison between the tailpipe and the CVS

Figure 3 showed the particle number concentration and size distribution as a function of cycle time for the Euro 6 G-DI vehicle during an Artemis motorway driving cycle after the tailpipe (Figure 3a) and after the CVS (Figure 3b). At the tailpipe, particle emissions were characterised by narrow peaks of about 5s mainly during accelerations (Figure 3a), while after CVS particle emissions were characterised by larger emission peaks of about 30s and were observed for the whole cycle length (Figure 3b). Particle size distribution after tailpipe varied between 2 nm and 70 nm with a main mode at 10 nm. After the CVS the particle size distribution was centred at 50 nm and no particles below 30 nm were detected. This observation indicated that condensation and possibly coagulation happened. We observed an increase in PN after the CVS suggesting that also nucleation occurred in the CVS tunnel.



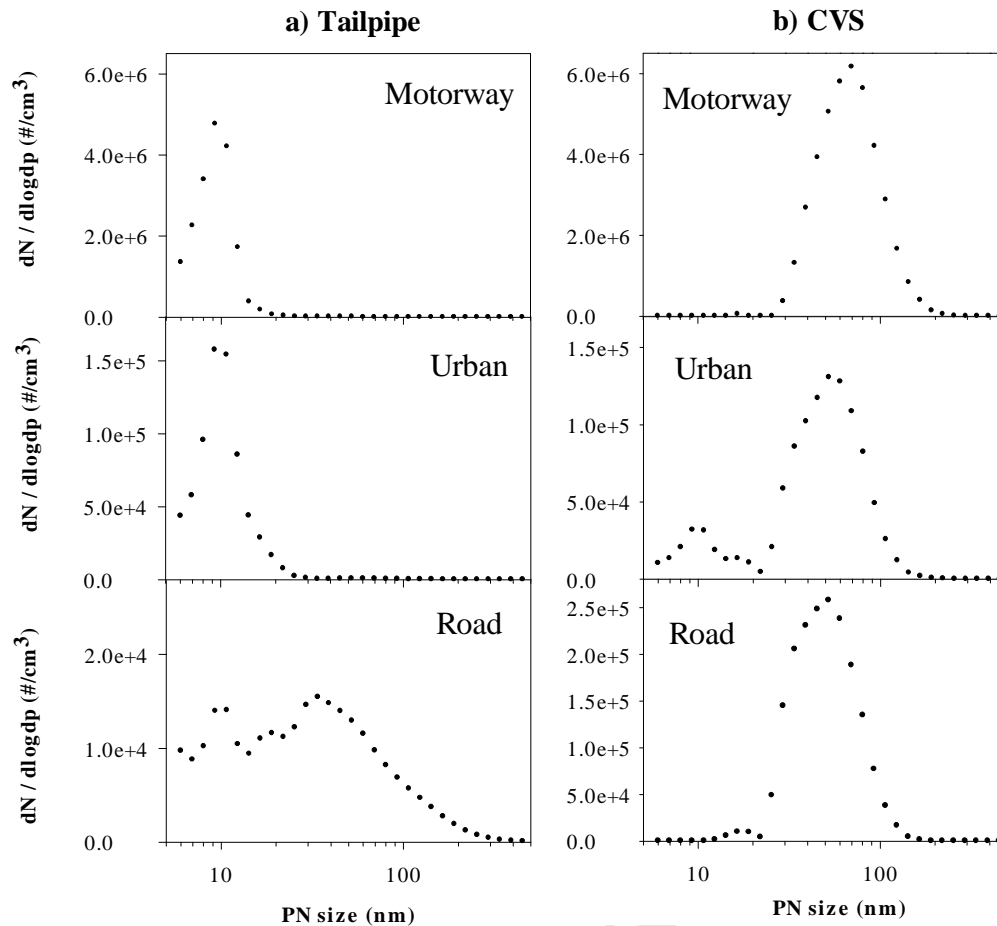
261



262

263 Figure 3. Particle number concentration of the G-DI vehicle during an Artemis motorway driving  
264 cycle, sampled: a) after the tailpipe and b) after the CVS. PN size distribution is described on the left  
265 Y-axis. The light blue line represents the vehicle speed (km/h) on the right Y-axis.

266 Vehicle accelerations lead to distinct emission peaks. An average of emissions over the whole  
267 cycle did not account for these disparities. In order to compare the CVS and exhaust particle size in an  
268 acceleration phase (high emission), we choose the highest emission peak for each cycle. Comparisons  
269 were made at 500s, 750s and 430s, respectively, for Artemis urban, road and motorway cycles. Figure  
270 4 showed the PN size distribution for these three driving conditions after the tailpipe (Figure 4a) and  
271 after the CVS (Figure 4b). For motorway, both tailpipe and CVS particle size distribution were  
272 unimodal. However, the CVS measurement showed a higher PN concentration with the particle  
273 diameter centred at 70 nm comparing to the tailpipe, for which the particle diameter was smaller and  
274 centred at 10 nm. For urban, particle size distribution after the tailpipe was similar than the motorway  
275 cycle, with a unimodal distribution centred at 10 nm. While after the CVS, the PN size distribution  
276 was bimodal with a main mode at 50 nm and a second lower mode at 10 nm. For road, the tailpipe  
277 particle size distribution was different than motorway and urban. It showed a bimodal distribution with  
278 two main modes at 10 nm and 30 nm, and the CVS particle size distribution was unimodal and centred  
279 at 50 nm. However, a similar increase in the particle diameter and concentration was observed in the  
280 CVS as two other driving conditions. This observation could be explained by the nucleation,  
281 condensation and coagulation phenomena as described by Seinfeld (2016). The increase in particle  
282 number highlighted that nucleation process happened in the CVS. Moreover, different precursors in  
283 vehicle exhaust, such as semi volatile compounds, sulfuric acid, ammonia, polycyclic aromatic  
284 hydrocarbons (PAH), hopanes and steranes, could cause the nucleation and induce an increase in small  
285 particle numbers (Louis et al., 2016; Benson et al., 2011; Casati et al., 2007; Virtanen et al., 2006;  
286 Burtscher, 2005; Mathis et al., 2005; Zielinska et al., 2004; Bukowiecki et al., 2003). The nucleation  
287 phenomenon has already been observed in other exhaust dilution studies by Vouitsis et al. (2009) and  
288 Kittelson et al. (1998 and 2000). On the other hand, the particle growth from 10 nm to 50 nm  
289 highlighted the condensation and coagulation phenomena that depended on the SVOCs and particle  
290 concentration in the exhaust. The SVOCs condensed to the particle surface as function of the partition  
291 coefficient between the gas and the particulate phase, which induced a rapid growth of the particles  
292 (Zhang et al., 2004). The work of Albriet et al. (2010), with an aerosol computational fluid dynamics  
293 model (CFD), confirmed that SVOCs condensation governed the growth of the nanoparticles in the  
294 tailpipe plume of vehicles.



295

296 Figure 4. Euro 6 G-DI particle size distribution: a) after tailpipe and b) after CVS for Artemis  
 297 motorway (at 430s), urban (at 500s) and road (at 750s). Data were measured by a Fast Mobility  
 298 Particle Sizer Spectrometer (FMPS).

299 For urban, we also observed a particle mode at 10 nm after CVS that could be explained by the  
 300 lower PN concentration and flow rate in the CVS than motorway (9 m<sup>3</sup>/min for urban and 11 m<sup>3</sup>/min  
 301 for motorway). According to Albriet et al. (2010), turbulence remains a crucial parameter for particle  
 302 growth. The CVS sampling system turbulence was calculated by the Reynolds number given by  
 303 Kulkarni (2011). Reynolds number determines if the gas flow was laminar ( $Re < 3 \times 10^3$ ) or turbulent  
 304 ( $Re > 3 \times 10^3$ ).

305

$$Re = \frac{U \times d}{\nu}$$

306 U: velocity characteristic of the gas (m/s)

307 d: diameter of the pipe (m)

308  $\nu$ : kinematic gas viscosity ( $\nu = \eta/\rho_g$ )

309 For the CVS sampling system, the Reynolds numbers were  $5 \times 10^4$ ,  $4 \times 10^4$  and  $4 \times 10^4$  for the  
 310 motorway, urban and road cycles respectively that were greater than the limit value ( $3 \times 10^3$ ). The CVS  
 311 flow was thus a turbulent flow that promoted the phenomena of condensation and coagulation as well  
 312 as the temporal diffusion of the PN concentration peaks. This turbulence was proportional to the  
 313 average cycle speed. Low turbulence for the urban condition together with low PN concentration  
 314 induced low coagulation and condensation rates compared to motorway condition, which could  
 315 explain the bimodal PN distribution in the CVS.

316 Furthermore, high particle concentration and turbulent flow added to the Brownian motion  
317 (random movement of a particle due to collisions with surrounding air particles) could induce  
318 turbulent coagulation (Huang et al., 2014; Zhang et al., 2004). Table 4 (Appendix) shows an example  
319 of particle coagulation time with different particle sizes and particle concentrations. The coagulation  
320 coefficients used in this work were taken from Seinfeld (2016) assuming that the particles were  
321 monodisperse taken into account the kinetic corrections and without turbulence. The coagulation half-  
322 life time ( $\tau_c$ ) was determined with the following equation:

$$\tau_c = \frac{2}{K \times N_0}$$

323 K: coagulation coefficient for monodisperse aerosols;

324  $N_0$ : particle concentration

325 For particles having mobility diameter at 10 nm, the coagulation times were 3, 100 and 1000  
326 minutes (Table 4, Appendix) for the concentration at  $5.5 \times 10^6 \text{ \#/cm}^3$ ,  $1.6 \times 10^5 \text{ \#/cm}^3$  and  $1.4 \times 10^4 \text{ \#/cm}^3$ ,  
327 respectively, which represented motorway, urban and road PN emissions (Figure 4). For the particles  
328 with diameter at 40 nm, the coagulation times were higher than 1000 minutes for all conditions.  
329 According to Albriet et al. (2010) and Grieshop et al. (2009a), coagulation by diffusion is a slow  
330 process that takes more than five minutes to occur, which is greater than the CVS residence time (2–10  
331 seconds). The turbulence of gas flow in the sampling system could reduce the coagulation time.  
332 However, coagulation is known to have a little impact on particle growth in the first seconds after the  
333 exhaust (Albriet et al., 2010). These results indicated that the CVS sampling system could induce  
334 nucleation and condensation phenomena influencing the particle characteristic and quantification.  
335 Particle sampling at the tailpipe could represent a complementary method to better quantify the  
336 particle emissions.



#### 337 **4 Conclusion**

338 To investigate the effects of the exhaust dilution on particle emissions, two types of  
339 experiments were performed on a chassis dynamometer: 1) dilution and temperature effects on particle  
340 emission were investigated with Euro 5 diesel and gasoline vehicles; 2) sampling condition impacts on  
341 particle quantification were investigated with Euro 6 diesel and gasoline vehicles. The dilution and  
342 temperature effects were studied directly from tailpipe with dilution ratios ranged from 8 to 4000 and  
343 dilution temperatures from 50°C to 150°C. Low dilution temperature and low dilution ratios increased  
344 the particle number concentration by a factor of 1.4–3. The results highlighted that the low primary  
345 dilution ratios induced a significant influence on particle number concentration. At low primary  
346 dilution (3–5), the particle emission was 2 times higher than at high primary dilution (12–20). To  
347 minimise the bias, the FPS sampling system at tailpipe should be set at high primary dilution and high  
348 dilution temperature.

349 In the second experiment, particle emissions from tailpipe were compared to those after the  
350 CVS system under similar dilution conditions with two Euro 6 vehicles (gasoline G-DI and diesel  
351 DPFcat). Due to the high efficiency of the diesel particulate filter, PN emissions from the Euro 6  
352 diesel vehicle were near the detection limit. For Euro 6 G-DI vehicle, CVS PN concentrations were  
353 higher than those at the tailpipe by a factor of 6, 80 and 22 for Artemis urban, road and motorway,  
354 respectively. The main particle size mode after the tailpipe was centred on 10 nm while, particle size  
355 after the CVS was centred at 70 nm for motorway and 50 nm for urban and road driving. The increase  
356 in PN concentration and the growth of particle size in the CVS were induced by the nucleation and  
357 condensation. These processes could be supported by different semi volatile particle precursors  
358 observed in our previous studies and by the turbulent flow in the sampling tunnel (Reynolds numbers  
359 =  $4-5 \times 10^4$ ). The coagulation could happen in the CVS because of the high PN concentration and  
360 turbulent flow, but it remained a negligible process for the short CVS residence time (2–10s). These  
361 results indicated that the CVS sampling system could induce an over-estimation of PN. Particle  
362 sampling at tailpipe could represent a complementary method to better quantify the particle emissions.

#### 363 **Acknowledgements**

364 The authors would like to thank the French Environment and Energy Management Agency (ADEME)  
365 for financial support of the CORTEA project CaPVeREA and the Auvergne Rhône-Alpes region.

366 **References**

- 367 Albriet, B., K.N. Sartelet, S. Lacour, B. Carissimo, and C. Seigneur. 'Modelling Aerosol Number Distributions  
368 from a Vehicle Exhaust with an Aerosol CFD Model'. *Atmospheric Environment* 44, no. 8 (March 2010):  
369 1126–37. doi:10.1016/j.atmosenv.2009.11.025.
- 370 André, Michel. 'The ARTEMIS European Driving Cycles for Measuring Car Pollutant Emissions.' *Science of*  
371 *The Total Environment* 334–35 (December 2004): 73–84. doi:10.1016/j.scitotenv.2004.04.070.
- 372 Beckers, J., W. W. Stoffels, and G. M. W. Kroesen. 'Temperature Dependence of Nucleation and Growth of  
373 Nanoparticles in Low Pressure Ar/CH<sub>4</sub> RF Discharges.' *Journal of Physics D: Applied Physics* 42, no.  
374 15 (2009): 155206. doi:10.1088/0022-3727/42/15/155206.
- 375 Benson, D. R., J. H. Yu, A. Markovich, and S.-H. Lee. 'Ternary Homogeneous Nucleation of H<sub>2</sub>SO<sub>4</sub>, NH<sub>3</sub>, and  
376 H<sub>2</sub>O under Conditions Relevant to the Lower Troposphere.' *Atmos. Chem. Phys.* 11, no. 10 (20 May  
377 2011): 4755–66. doi:10.5194/acp-11-4755-2011.
- 378 Bukowiecki, N., J. Dommen, A. S. H. Prévôt, E. Weingartner, and U. Baltensperger. 'Fine and Ultrafine  
379 Particles in the Zürich (Switzerland) Area Measured with a Mobile Laboratory: An Assessment of the  
380 Seasonal and Regional Variation throughout a Year.' *Atmos. Chem. Phys.* 3, no. 5 (24 September 2003):  
381 1477–94. doi:10.5194/acp-3-1477-2003.
- 382 Burtscher, H. 'Physical Characterization of Particulate Emissions from Diesel Engines: A Review.' *Journal of*  
383 *Aerosol Science* 36, no. 7 (July 2005): 896–932. doi:10.1016/j.jaerosci.2004.12.001.
- 384 Casati, Roberto, Volker Scheer, Rainer Vogt, and Thorsten Benter. 'Measurement of Nucleation and Soot Mode  
385 Particle Emission from a Diesel Passenger Car in Real World and Laboratory in Situ Dilution.'  
386 *Atmospheric Environment* 41, no. 10 (March 2007): 2125–35. doi:10.1016/j.atmosenv.2006.10.078.
- 387 Fujitani, Yuji, Katsumi Saitoh, Akihiro Fushimi, Katsuyuki Takahashi, Shuich Hasegawa, Kiyoshi Tanabe,  
388 Shinji Kobayashi, Akiko Furuyama, Seishiro Hirano, and Akinori Takami. 'Effect of Isothermal Dilution  
389 on Emission Factors of Organic Carbon and N-Alkanes in the Particle and Gas Phases of Diesel Exhaust.'  
390 *Atmospheric Environment* 59 (November 2012): 389–97. doi:10.1016/j.atmosenv.2012.06.010.
- 391 Giechaskiel, Barouch, Matti Maricq, Leonidas Ntziachristos, Christos Dardiotis, Xiaoliang Wang, Harald  
392 Axmann, Alexander Bergmann, and Wolfgang Schindler. 'Review of Motor Vehicle Particulate  
393 Emissions Sampling and Measurement: From Smoke and Filter Mass to Particle Number'. *Journal of*  
394 *Aerosol Science* 67 (January 2014): 48–86. doi:10.1016/j.jaerosci.2013.09.003.
- 395 Giechaskiel, B., R. Chirico, P.F. DeCarlo, M. Clairotte, T. Adam, G. Martini, M.F. Heringa, R. Richter, A.S.H.  
396 Prevot, and U. Baltensperger. 'Evaluation of the Particle Measurement Programme (PMP) Protocol to  
397 Remove the Vehicles' Exhaust Aerosol Volatile Phase.' *Science of The Total Environment* 408, no. 21 (1  
398 October 2010): 5106–16. doi:10.1016/j.scitotenv.2010.07.010.
- 399 Giechaskiel, Barouch, Panagiota Dilara, and Jon Andersson. 'Particle Measurement Programme (PMP) Light-  
400 Duty Inter-Laboratory Exercise: Repeatability and Reproducibility of the Particle Number Method'.  
401 *Aerosol Science and Technology* 42, no. 7 (29 May 2008): 528–43. doi:10.1080/02786820802220241.
- 402 Giechaskiel, B., L. Ntziachristos, Z. Samaras, and R. Casati. 'Effect of Speed and Speed-Transition on the  
403 Formation of Nucleation Mode Particles from a Light Duty Diesel Vehicle', 2007, 15. doi:10.4271/2007-  
404 01-1110.
- 405 Grieshop, Andrew P., Marissa A. Miracolo, Neil M. Donahue, and Allen L. Robinson. 'Constraining the  
406 Volatility Distribution and Gas-Particle Partitioning of Combustion Aerosols Using Isothermal Dilution  
407 and Thermodynamic Measurements.' *Environmental Science & Technology* 43, no. 13 (1 July 2009):  
408 4750–56. doi:10.1021/es8032378.
- 409 Grieshop, A. P., J. M. Logue, N. M. Donahue, and A. L. Robinson. 'Laboratory Investigation of Photochemical  
410 Oxidation of Organic Aerosol from Wood Fires 1: Measurement and Simulation of Organic Aerosol  
411 Evolution.' *Atmos. Chem. Phys.* 9, no. 4 (18 February 2009): 1263–77. doi:10.5194/acp-9-1263-2009.
- 412 Huang, L., S. L. Gong, M. Gordon, J. Liggio, R. Staebler, C. A. Stroud, G. Lu, C. Mihele, J. R. Brook, and C. Q.  
413 Jia. 'Aerosol-computational Fluid Dynamics Modeling of Ultrafine and Black Carbon Particle Emission,  
414 Dilution, and Growth near Roadways.' *Atmos. Chem. Phys.* 14, no. 23 (2 December 2014): 12631–48.  
415 doi:10.5194/acp-14-12631-2014.
- 416 Jamriska, Milan, Lidia Morawska, Steven Thomas, and Congrong He. 'Diesel Bus Emissions Measured in a  
417 Tunnel Study.' *Environmental Science & Technology* 38, no. 24 (1 December 2004): 6701–9.  
418 doi:10.1021/es030662z.
- 419 Karjalainen, Panu, Liisa Pirjola, Juha Heikkilä, Tero Lähde, Theodoros Tzamkiozis, Leonidas Ntziachristos,  
420 Jorma Keskinen, and Topi Rönkkö. 'Exhaust Particles of Modern Gasoline Vehicles: A Laboratory and an  
421 on-Road Study.' *Atmospheric Environment* 97 (November 2014): 262–70.  
422 doi:10.1016/j.atmosenv.2014.08.025.
- 423 Kim, Youngseob, Karine Sartelet, Christian Seigneur, Aurélie Charron, Jean-Luc Besombes, Jean-Luc Jaffrezo,  
424 Nicolas Marchand, and Lucie Polo. 'Effect of Measurement Protocol on Organic Aerosol Measurements

- 425 of Exhaust Emissions from Gasoline and Diesel Vehicles.' *Atmospheric Environment* 140 (September  
426 2016): 176–87. doi:10.1016/j.atmosenv.2016.05.045.
- 427 Kittelson, David B. 'Engines and Nanoparticles : A Review.' *Journal of Aerosol Science* 29, no. 5/6 (1998):  
428 575–88. doi:0021-8502/98.
- 429 Kittelson, David, Jason Johnson, and Winthrop Watts. 'Diesel Aerosol Sampling in the Atmosphere.' San Diego,  
430 California, 2000. <http://papers.sae.org/2000-01-2212/>.
- 431 Köhler, Felix. 'Testing of Particulate Emissions from Positive Ignition Vehicles with Direct Fuel Injection  
432 System.' Technical Report, 2013-09-26, T\HuV Nord, 2013.  
433 [http://www.transportenvironment.org/sites/te/files/publications/TUV-Technical\\_report.pdf](http://www.transportenvironment.org/sites/te/files/publications/TUV-Technical_report.pdf).
- 434 Kozawa, Kathleen H., Arthur M. Winer, and Scott A. Fruin. 'Ultrafine Particle Size Distributions near Freeways:  
435 Effects of Differing Wind Directions on Exposure.' *Atmospheric Environment* 63 (December 2012):  
436 250–60. doi:10.1016/j.atmosenv.2012.09.045.
- 437 Kulkarni, Pramod, Paul A. Baron, and Klaus Willeke. *Aerosol Measurement: Principles, Techniques, and*  
438 *Applications*. John Wiley & Sons, 2011.
- 439 Kulmala, Markku, Liisa Pirjola, and Jyrki M. Mäkelä. 'Stable Sulphate Clusters as a Source of New  
440 Atmospheric Particles.' *Nature* 404, no. 6773 (2 March 2000): 66–69. doi:10.1038/35003550.
- 441 Liang, Bin, Yunshan Ge, Jianwei Tan, Xiukun Han, Liping Gao, Lijun Hao, Wentao Ye, and Peipei Dai.  
442 'Comparison of PM Emissions from a Gasoline Direct Injected (GDI) Vehicle and a Port Fuel Injected  
443 (PFI) Vehicle Measured by Electrical Low Pressure Impactor (ELPI) with Two Fuels: Gasoline and M15  
444 Methanol Gasoline.' *Journal of Aerosol Science* 57 (March 2013): 22–31.  
445 doi:10.1016/j.jaerosci.2012.11.008.
- 446 Louis, Cédric, Yao Liu, Patrick Tassel, Pascal Perret, Agnès Chaumond, and Michel André. 'PAH, BTEX,  
447 Carbonyl Compound, Black-Carbon, NO<sub>2</sub> and Ultrafine Particle Dynamometer Bench Emissions for  
448 Euro 4 and Euro 5 Diesel and Gasoline Passenger Cars.' *Atmospheric Environment* 141 (September  
449 2016): 80–95. doi:10.1016/j.atmosenv.2016.06.055.
- 450 Mamakos, Athanasios, and Giorgio Martini. 'Particle Number Emissions During Regeneration of DPF-Equipped  
451 Light Duty Diesel Vehicles', 2011.
- 452 Manoukian, A., D. Buiron, B. Temime-Roussel, H. Wortham, and E. Quivet. 'Measurements of VOC/SVOC  
453 Emission Factors from Burning Incenses in an Environmental Test Chamber: Influence of Temperature,  
454 Relative Humidity, and Air Exchange Rate.' *Environmental Science and Pollution Research* 23, no. 7  
455 (April 2016): 6300–6311. doi:10.1007/s11356-015-5819-2.
- 456 Mathis, U, M Mohr, and A Forss. 'Comprehensive Particle Characterization of Modern Gasoline and Diesel  
457 Passenger Cars at Low Ambient Temperatures.' *Atmospheric Environment* 39, no. 1 (January 2005):  
458 107–17. doi:10.1016/j.atmosenv.2004.09.029.
- 459 Mathis, Urs, Jyrki Ristimäki, Martin Mohr, Jorma Keskinen, Leonidas Ntziachristos, Zissis Samaras, and Pirta  
460 Mikkänen. 'Sampling Conditions for the Measurement of Nucleation Mode Particles in the Exhaust of a  
461 Diesel Vehicle.' *Aerosol Science and Technology* 38, no. 12 (January 2004): 1149–60.  
462 doi:10.1080/027868290891497.
- 463 May, Andrew A., Albert A. Presto, Christopher J. Hennigan, Ngoc T. Nguyen, Timothy D. Gordon, and Allen L.  
464 Robinson. 'Gas-Particle Partitioning of Primary Organic Aerosol Emissions: (1) Gasoline Vehicle  
465 Exhaust.' *Atmospheric Environment* 77 (October 2013): 128–39. doi:10.1016/j.atmosenv.2013.04.060.
- 466 Morawska, L., Z. Ristovski, E.R. Jayaratne, D.U. Keogh, and X. Ling. 'Ambient Nano and Ultrafine Particles  
467 from Motor Vehicle Emissions: Characteristics, Ambient Processing and Implications on Human  
468 Exposure.' *Atmospheric Environment* 42, no. 35 (November 2008): 8113–38.  
469 doi:10.1016/j.atmosenv.2008.07.050.
- 470 Ning, Zhi. 'Atmospheric Processes Influencing Aerosols Generated by Combustion and the Inference of Their  
471 Impact on Public Exposure: A Review.' *Aerosol and Air Quality Research*, 2010.  
472 doi:10.4209/aaqr.2009.05.0036.
- 473 Pope III, C. Arden. 'Review: Epidemiological Basis for Particulate Air Pollution Health Standards.' *Aerosol*  
474 *Science & Technology* 32, no. 1 (2000): 4–14.
- 475 Ranjan, Manish, Albert A. Presto, Andrew A. May, and Allen L. Robinson. 'Temperature Dependence of Gas-  
476 Particle Partitioning of Primary Organic Aerosol Emissions from a Small Diesel Engine.' *Aerosol*  
477 *Science and Technology* 46, no. 1 (1 January 2012): 13–21. doi:10.1080/02786826.2011.602761.
- 478 Rönkkö, Annele Virtanen. 'Effect of Dilution Conditions and Driving Parameters on Nucleation Mode Particles  
479 in Diesel Exhaust: Laboratory and on-Road Study.' *Atmospheric Environment* 40, no. 16 (2006): 2893–  
480 2901. doi:10.1016/j.atmosenv.2006.01.002.
- 481 Seinfeld, John H., and Spyros N. Pandis. *Atmospheric Chemistry and Physics: From Air Pollution to Climate*  
482 *Change*. John Wiley & Sons, 2016.
- 483 Uhrner, Ulrich, Michael Zallinger, Sibylle von Löwis, Hanna Vehkamäki, Birgit Wehner, Frank Stratmann, and  
484 Alfred Wiedensohler. 'Volatile Nanoparticle Formation and Growth within a Diluting Diesel Car

- 485 Exhaust.' *Journal of the Air & Waste Management Association* 61, no. 4 (April 2011): 399–408.  
486 doi:10.3155/1047-3289.61.4.399.
- 487 Virtanen, A., T. Rönkkö, J. Kannosto, J. Ristimäki, J. M. Mäkelä, J. Keskinen, T. Pakkanen, R. Hillamo, L.  
488 Pirjola, and K. Hämeri. 'Winter and Summer Time Size Distributions and Densities of Traffic-Related  
489 Aerosol Particles at a Busy Highway in Helsinki.' *Atmospheric Chemistry and Physics* 6, no. 9 (2006):  
490 2411–21.
- 491 Vouitsis, Elias, Leonidas Ntziachristos, Panayiotis Pistikopoulos, Zissis Samaras, Loukia Chrysikou, Constantini  
492 Samara, Chrysi Papadimitriou, Petros Samaras, and George Sakellaropoulos. 'An Investigation on the  
493 Physical, Chemical and Ecotoxicological Characteristics of Particulate Matter Emitted from Light-Duty  
494 Vehicles.' *Environmental Pollution* 157, no. 8–9 (August 2009): 2320–27.  
495 doi:10.1016/j.envpol.2009.03.028.
- 496 Vouitsis, Elias, Leonidas Ntziachristos, and Zissis Samaras. 'Theoretical Investigation of the Nucleation Mode  
497 Formation Downstream of Diesel after-Treatment Devices.' *Aerosol and Air Quality Research* 8, no. 1  
498 (2008): 37–53.
- 499 Wang, Yan Jason, and K. Max Zhang. 'Coupled Turbulence and Aerosol Dynamics Modeling of Vehicle  
500 Exhaust Plumes Using the CTAG Model.' *Atmospheric Environment* 59 (November 2012): 284–93.  
501 doi:10.1016/j.atmosenv.2012.04.062.
- 502 Wei, Wenjuan, Corinne Mandin, Olivier Blanchard, Fabien Mercier, Maud Pelletier, Barbara Le Bot, Philippe  
503 Glorennec, and Olivier Ramalho. 'Temperature Dependence of the Particle/gas Partition Coefficient: An  
504 Application to Predict Indoor Gas-Phase Concentrations of Semi-Volatile Organic Compounds.' *Science  
505 of The Total Environment* 563–64 (1 September 2016): 506–12. doi:10.1016/j.scitotenv.2016.04.106.
- 506 Zhang, K. Max, and Anthony S. Wexler. 'Evolution of Particle Number Distribution near roadways—Part I:  
507 Analysis of Aerosol Dynamics and Its Implications for Engine Emission Measurement.' *Atmospheric  
508 Environment* 38, no. 38 (December 2004): 6643–53. doi:10.1016/j.atmosenv.2004.06.043.
- 509 Zhang, K. Max, Anthony S. Wexler, Yi Fang Zhu, William C. Hinds, and Constantinos Sioutas. 'Evolution of  
510 Particle Number Distribution near Roadways. Part II: The "Road-to-Ambient" Process'. *Atmospheric  
511 Environment* 38, no. 38 (December 2004): 6655–65. doi:10.1016/j.atmosenv.2004.06.044.
- 512 Zielinska, Barbara, John Sagebiel, Jacob D. McDonald, Kevin Whitney, and Douglas R. Lawson.  
513 'Emission Rates and Comparative Chemical Composition from Selected in-Use Diesel and  
514 Gasoline-Fueled Vehicles.' *Journal of the Air & Waste Management Association* 54, no. 9  
515 (2004): 1138–50.

516 **Appendix**

517 Table 4. CVS coagulation time for monodisperse particles as function of the PN size and  
 518 concentration. The coagulation coefficient takes into account the kinetic corrections but not the  
 519 turbulence.

Driving Cycle	PN size (nm)	PN concentration (#/cm <sup>3</sup> )	Coagulation coefficient (cm <sup>3</sup> /s)	Coagulation time (s)
Motorway	4	$1.3 \times 10^6$	$1.3 \times 10^{-9}$	$1.2 \times 10^3$
	10	$5.5 \times 10^6$	$1.9 \times 10^{-9}$	$1.9 \times 10^2$
	20	$1.5 \times 10^6$	$2.4 \times 10^{-9}$	$5.4 \times 10^2$
	40	$4.8 \times 10^3$	$2.3 \times 10^{-9}$	$1.8 \times 10^5$
	100	$1.6 \times 10^3$	$1.5 \times 10^{-9}$	$8.1 \times 10^5$
Urban	4	$4.4 \times 10^4$	$1.3 \times 10^{-9}$	$3.5 \times 10^4$
	10	$1.6 \times 10^5$	$1.9 \times 10^{-9}$	$6.7 \times 10^3$
	20	$1.7 \times 10^4$	$2.4 \times 10^{-9}$	$5.0 \times 10^4$
	40	$5.2 \times 10^2$	$2.3 \times 10^{-9}$	$1.7 \times 10^6$
	100	$2.5 \times 10^2$	$1.5 \times 10^{-9}$	$5.5 \times 10^6$
Road	4	$9.7 \times 10^3$	$1.3 \times 10^{-9}$	$1.6 \times 10^5$
	10	$1.4 \times 10^4$	$1.9 \times 10^{-9}$	$7.5 \times 10^4$
	20	$1.2 \times 10^4$	$2.4 \times 10^{-9}$	$7.2 \times 10^4$
	40	$1.5 \times 10^4$	$2.3 \times 10^{-9}$	$5.9 \times 10^4$
	100	$5.7 \times 10^3$	$1.5 \times 10^{-9}$	$2.4 \times 10^5$

520

521 **Table of Contents**

522 **Tables**

523 Table 1. Technical characteristics of the tested vehicles..... 4  
524 Table 2. Detailed driving cycles with repeated tests number and sampling conditions for the FPS and  
525 the CVS with Euro 6 G-DI (No.3) and Euro 6 diesel DPF cat (No.4) vehicles. .... 6  
526 Table 3. Average particle number concentration for G-DI Euro 6 vehicle. .... 10  
527 Table 4. CVS coagulation time for monodisperse particles as function of the PN size and  
528 concentration. The coagulation coefficient takes into account the kinetic corrections but not the  
529 turbulence..... 18  
530

531 **Figures**

532 Figure 1. Schema of the experimental setup; the green arrows represent the CVS way and the red  
533 arrows represent the direct tailpipe way with FPS dilution..... 5  
534 Figure 2. Total dilution and temperature effects (a) and primary dilution and temperature effects (b)  
535 for the gasoline Euro 5 vehicle (No. 1) during the motorway driving conditions, at 50°C, 100°C and  
536 150°C. The particle number emissions are corrected taking into account of the dilution factors. For the  
537 figure 2b, the black dots show total dilution ratios at 30, 400, 2000 and 4000 with low primary dilution  
538 (3–5) and the white dots show total dilution ratios at 100 and 1000 with high primary dilution (12–20).  
539 ..... 9  
540 Figure 3. Particle number concentration of the G-DI vehicle during an Artemis motorway driving  
541 cycle, sampled: a) after the tailpipe and b) after the CVS. PN size distribution is described on the left  
542 Y-axis. The light blue line represents the vehicle speed (km/h) on the right Y-axis. .... 11  
543 Figure 4. Euro 6 G-DI particle size distribution: a) after tailpipe and b) after CVS for Artemis  
544 motorway (at 430s), urban (at 500s) and road (at 750s). Data were measured by a Fast Mobility  
545 Particle Sizer Spectrometer (FMPS). .... 12  
546

## Highlights

- Dilution and temperature effects on particle number emission
- Comparison between tailpipe and CVS for particle number emission
- Over-emission of particles from the CVS because of nucleation, condensation and coagulation
- Tailpipe measurement as a complementary method to the CVS for exhaust particle sampling